Cu₂S nanowires and MnS/Cu₂S nanojunctions derived from γ-MnS nanowires via selective cation-exchange reaction

G. Xu[1,2], Y. L. Zhu[1], and X. L. Ma*[,1]

[1] Shenyang National Laboratory for Materials Science, Institute of Metal Research, Chinese Academy of Sciences, 110016 Shenyang, P.R. China
[2] School of Science, Shenyang University of Technology, 110870 Shenyang, P.R. China

* Corresponding author: e-mail xlma@imr.ac.cn, Phone: +86-24-23971845, Fax: +86-24-23971215

Cu₂S nanowires and MnS/Cu₂S junctions have been derived on the basis of γ-MnS nanowires via cation-exchange reaction. Relationships between a selective cation exchange and the growth direction of the γ-MnS nanowires are identified by means of transmission electron microscopy. In the case of γ-MnS nanowires with [0001] growth direction, Cu⁺ exchange with an initial γ-MnS nanowire results in a Cu₂S nanowire. In contrast, for γ-MnS nanowires with [1–100] growth direction, Cu⁺ exchange leads to a striped MnS/Cu₂S junction. Mechanisms for this selective cation exchange are proposed.

1 Introduction One-dimensional (1D) nanoscale building blocks, such as nanowires and nanorods, are of great importance for both fundamental research and potential applications. Controllable synthesis of 1D nanostructures may provide great opportunities for exploring their novel properties and for fabrication of potential nanodevices [1]. Among 1D nanostructures, 1D heterostructures in the axial direction with modulated compositions have received much attention, which can be synthesized by various methods, for example, vapor–liquid–solid (VLS) growth, vapor–solid process, electrochemical deposition in templates, etc. [2]. In comparison, chemical conversions of one solid into another via insertion and exchange of ions are especially appealing because of the mild reaction conditions, potential for scaling up, and controllable factors. Cation-exchange reaction is a new approach to synthesis of partially or completely replaced nanostructures. This reaction has been successfully exploited for the preparation of nanocrystals [3–8], nanowires [9], superlattices [10], and core–shell nanoparticles [11, 12]. Moreover, it is found that nanomaterials with anisotropic shapes provide a platform for selective chemical modification based on the relative reactivities of different crystalline planes exposed at the surface [13]. Different reactivities on specific planes of nanostructures are available to selectively synthesis of multicomponent heterostructures through cation-exchange reaction, in which the kinetics and thermodynamics of the reaction are of the great concern [14].

Here, we report that the synthesis of Cu₂S nanowires and MnS/Cu₂S heterostructures based on the γ-MnS nanowires via selective cation-exchange reaction in 1.0 mol/L NaCl aqueous solution at ambient temperature. The chemical composition and microstructures of the products were characterized by means of transmission electron microscopy (TEM). We demonstrate that Cu⁺ substitution for Mn²⁺ is selective for γ-MnS nanowires with [0001] and [1–100] growth direction. This selectivity is mainly attributed to different Cu⁺ diffusion rates along different growth directions of the γ-MnS nanowires.

2 Experimental Mn(CH₃COO)₂ and SC(NH₂)₂ were selected as the manganese and sulfur sources, and ethylenediamine was used as the background reagent and for pH-value adjustment. All of the analytical grade chemicals were made by Sinopharm Chemical Reagent Co. Ltd., and were used without any further purification in the present study.

Synthesis of γ-MnS nanowires: γ-MnS nanowires were prepared by a hydrothermal method. First, 0.245 g Mn(CH₃COO)₂ and 10 ml ethylenediamine were added into a Teflon-lined autoclave, then the autoclave was filled with

50 ml distilled water, and finally 0.6 g SC(NH$_2$)$_2$ was added into the solution. The autoclave was sealed and heated in an electric oven at 120 °C for 18 h, and cooled in air to ambient temperature. Products were collected by centrifugation and cleaned with distilled water and ethanol for several times to remove impurities, and finally dried in air. The products for TEM observation were suspended in ethanol and dispersed by ultrasonication. A few drops of the fine particle suspension were deposited onto a carbon-coated copper grid.

Cation exchange of γ-MnS nanowires: After the first-round TEM observation, the copper grid specimen with the dispersed products was immersed into 1.0 mol/L NaCl aqueous solution for 20 h at room temperature. As reported previously, copper grids as a copper source have been effectively utilized to synthesize Cu$_2$S nanowire arrays [15] and Cu$_2$S nanowires [16]. The cation-exchange reaction was done under ambient conditions by mixing MnS nanowires with an excess amount of metal Cu in NaCl aqueous solution. The TEM specimen that experienced the cation exchange test was quickly cleaned (in distilled water and ethanol), dried, and transferred into the TEM for further investigation.

Microstructural characterization: Phase determination was performed with a JEM-2010 electron microscope (JEOL Ltd., Japan). High-resolution imaging, high-angle annular dark-field (HAADF) images, energy-filtered TEM (EFTEM) and energy-dispersive X-ray (EDS) spectra were carried out in a Tecnai G^2 F30 FEG transmission electron microscope (FEI Co., USA). The X-ray diffraction (XRD) measurements were done on an X-ray powder diffractometer (RIGAKU D/MAX 2500PC, Japan) with Cu Kα radiation by dispersing the powders on vaseline for adhesion.

3 Results Figure 1 shows an XRD pattern of the hydrothermal reaction products, and the main diffraction peaks can be clearly indexed to wurtzite MnS structure ($a = 0.388$ nm and $c = 0.638$ nm, space group $P6_3mc$). In the present work, the samples are not a single phase. A small quantity of residual Mn(CH$_3$COO)$_2$ and α-MnS phase

co-mixed with γ-MnS phase exist in the samples. Figure 2a is a bright-field TEM image showing the typical morphology of the as-received wire-like products. TEM images at higher magnification indicate that the nanowires are actually in bundles, as shown in Fig. 2b and the inset. HRTEM image (Fig. 2c) combined with fast Fourier transform (FFT) pattern (the inset in Fig. 2c) verifies the products are hexagonal γ-MnS nanowires with [0001] growth direction (named [0001] nanowires hereafter). The measured interplanar spacings, ∼0.635 and ∼0.330 nm, respectively, correspond to (0001) and (01–10) lattice planes of hexagonal MnS. In addition, γ-MnS nanowires with [1–100] growth direction (named [1–100] nanowires hereafter) are also identified, as shown in Fig. 2d and e. Two types of γ-MnS nanowires were found to coexist in the samples prepared by hydrothermal synthesis.

It is known that γ-MnS is a highly anisotropic crystal composed of covalently bound layers of Mn–S held together by much weaker van der Waals bonding. The atomic configuration of this layered structure is illustrated schematically in Fig. 2f. It is seen that the {0001} layers are stacked along the [0001] direction. Based on this configuration, the growth direction of the [1–100] nanowires is parallel to the (0001) layer, while in [0001] nanowires the growth direction is perpendicular to the (0001) layer. The [0001] nanowire exhibits a hexagonal cross-section and the sides of the wire

Figure 1 X-ray diffraction pattern of as-prepared samples by hydrothermal synthesis; the peaks marked by # result from γ-MnS structure, the peaks marked by ▲ result from α-MnS phase, and the peaks marked by ■ result from monoclinic Mn(CH$_3$COO)$_2$.
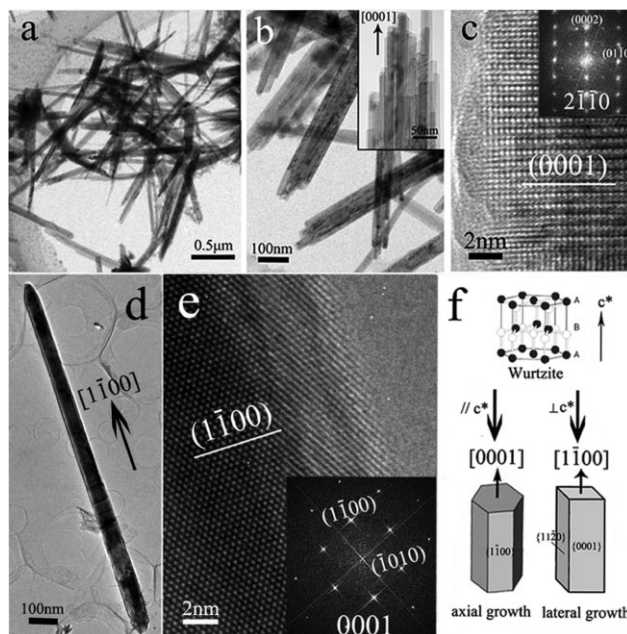
Figure 2 (a) Low-magnification TEM image of γ-MnS nanowire bundles; (b) enlarged part of (a) and zoom-in TEM image of the tips of these nanowires as an inset of (b); (c) HRTEM image and its corresponding FFT pattern (inset) of [0001] γ-MnS nanowire; (d) TEM image of a single [1–100] γ-MnS nanowire; (e) HRTEM image and its corresponding FFT pattern (inset) of the [1–100] γ-MnS nanowire; (f) atomic configuration of γ-MnS wurtzite crystal and schematic illustration of 1D γ-MnS nanowires with growth directions of [0001] and [1–100], respectively.

Phys. Status Solidi A **208**, No. 1 (2011)

125

Original

Paper
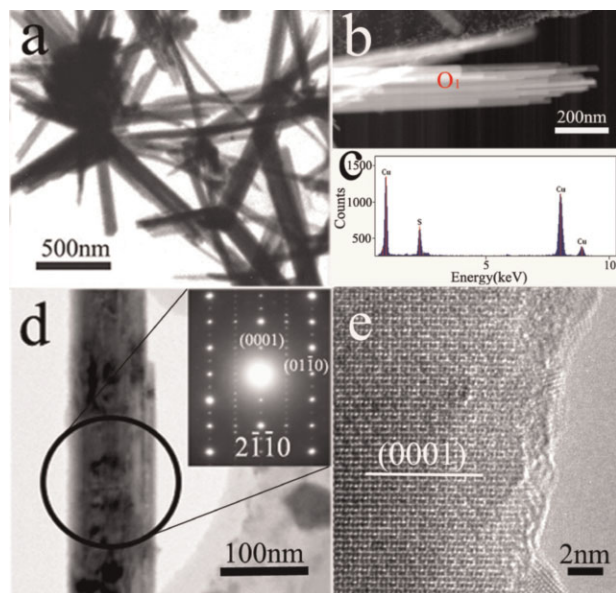
Figure 3 (online color at: www.pss-a.com) (a) TEM image of Cu_2S nanowire bundles; (b) HAADF image of a bundle of Cu_2S nanowires; (c) EDS spectrum of the region marked with red point 1 in (b); (d) TEM image of a bundle of Cu_2S nanowires, the inset is an SAED pattern taken in the region marked with the black circle; (e) HRTEM image of the Cu_2S nanowire.

are {1–100} faces. In contrast, the [1–100] nanowire has a rectangular cross-section and the sides of the wire are alternating ±(11–20) and ±(0001) planes, which is similar to the ZnO nanobelt [17].

After TEM observation on the as-synthesized MnS products, the copper grid specimen with the dispersed nanowires was immersed into 1.0 mol/L NaCl aqueous solution for 20 h at room temperature and then the second-round TEM study was performed. Structural evolution was found to be a function of the growth directions of the primary nanowires. Figure 3a shows a TEM image of the nanowire bundles synthesized by cation-exchange reaction. It can be seen that the geometry and size of the nanowires are all unchanged, compared with the primary ones as shown in Fig. 2a. Figure 3b is an HAADF image showing the morphology of a selected nanowire bundle. HAADF mode in a TEM provides incoherent images, which collects the high-angle scattered electrons and leads to strong atomic number (Z) contrast. The intensity of atom columns directly reflects their mean square atomic numbers; therefore the contrast in such a mode is strongly associated with chemical composition. The contrast is nearly uniform, indicating that the composition is homogeneous. The EDS spectrum shown in Fig. 3c reveals the presence of only copper and sulfur. Selected-area electron diffraction (SAED) pattern (the inset of Fig. 3d) combined with above the HAADF image and EDS analysis indicates that these Cu_2S nanowires are derived from the primary γ-MnS nanowires via the cation-exchange reaction. The Cu_2S nanowires also grow along the [0001] direction. The HRTEM image shown in Fig. 3e reveals

lattice fringes with an interfringe distance of $\sim$0.673 nm, matching fairly well with the {0001} planes of hexagonal Cu_2S ($a = 0.395$ nm and $c = 0.675$ nm, space group $P6_3/mmc$). Therefore, a complete conversion from the [0001] γ-MnS nanowire to the hexagonal Cu_2S nanowires took place through cation-exchange reaction, implying a complete replacement of Mn^{2+} in [0001] γ-MnS nanowires by Cu^+. Similar cases have been found in the CdS-Cu_2S binary nanorods [13], PtPb/Pt/PtPb nanowires [18], and CdS|PbS nanoheterostructures [19]. In this SAED pattern, extra weak spots with regular arrangement along the c^*-direction are found, which implies the formation of a long-period order structure in the Cu_2S nanowires.

In contrast, [1–100] γ-MnS nanowires show remarkable features after cation-exchange reaction, from which MnS/Cu_2S heterostructures were derived. Figure 4a shows a low magnification HAADF image of the heterostructures. Contrast fluctuation along the growth direction of the 1D nanostructures is also clearly seen. The area with bright contrast in an HAADF image implies the richness of heavy elements. Detailed analysis on the composition distribution in the heterostructure was carried out by means of EDS line scanning. The scanning route is marked with a red line in Fig. 4a. This scan begins from the tip 1, and goes across the interfaces and segments, finally ends at the tip 2. The plots of fluctuation along this line are given in Fig. 4b. It is seen that the alternating changing of contrast corresponds to the fluctuation of Mn/Cu content. Figure 4c–f are EFTEM images of the MnS/Cu_2S junction, in which copper, manganese, and sulfur are, respectively, selected to be imaged. The sulfur anion sublattice remains constant but manganese is partially replaced by copper in the cation-exchange process. The spatial distribution of these elements along the long axis of 1D nanostructures indicates that a MnS/Cu_2S junction is derived from the [1–100] γ-MnS nanowire via the cation-exchange reaction. The formation of this nanojunction is a remarkable feature for the [1–100] γ-MnS nanowire. In addition, it is of interest to note that there is strong contrast between two segments parallel to each other along the rod axis as seen in Fig. 4a and c. The appearance of such a contrast is believed to result from the facet morphology with rectangular cross-section as shown schematically in Fig. 2f. Such a contrast is invisible when the nanowire is imaged along [0001] zone axis, as seen in Fig. 2d, since in this case, the ±(11–20) lateral planes are edge-on.

Figure 5a is a TEM image of a typical heterostructure with a diameter of about 100 nm. Figure 5b is an EDP corresponding to the area marked with the black circle in Fig. 5a. This pattern is indexed as a superposition of $[11–23]_{MnS}$ and $[11–23]_{Cu_2S}$ zone axes. From this pattern, the orientation relationships between MnS and Cu_2S can be established as $(1–100)_{Cu_2S}//(1–100)_{MnS}$, and $[11–23]_{Cu_2S}//[11–23]_{MnS}$. Spot splitting (particularly for the high-indexed spots) is due to the difference of lattice parameters between γ-MnS and Cu_2S. Besides the strong diffraction spots from MnS and Cu_2S segments, extra spots marked by the white
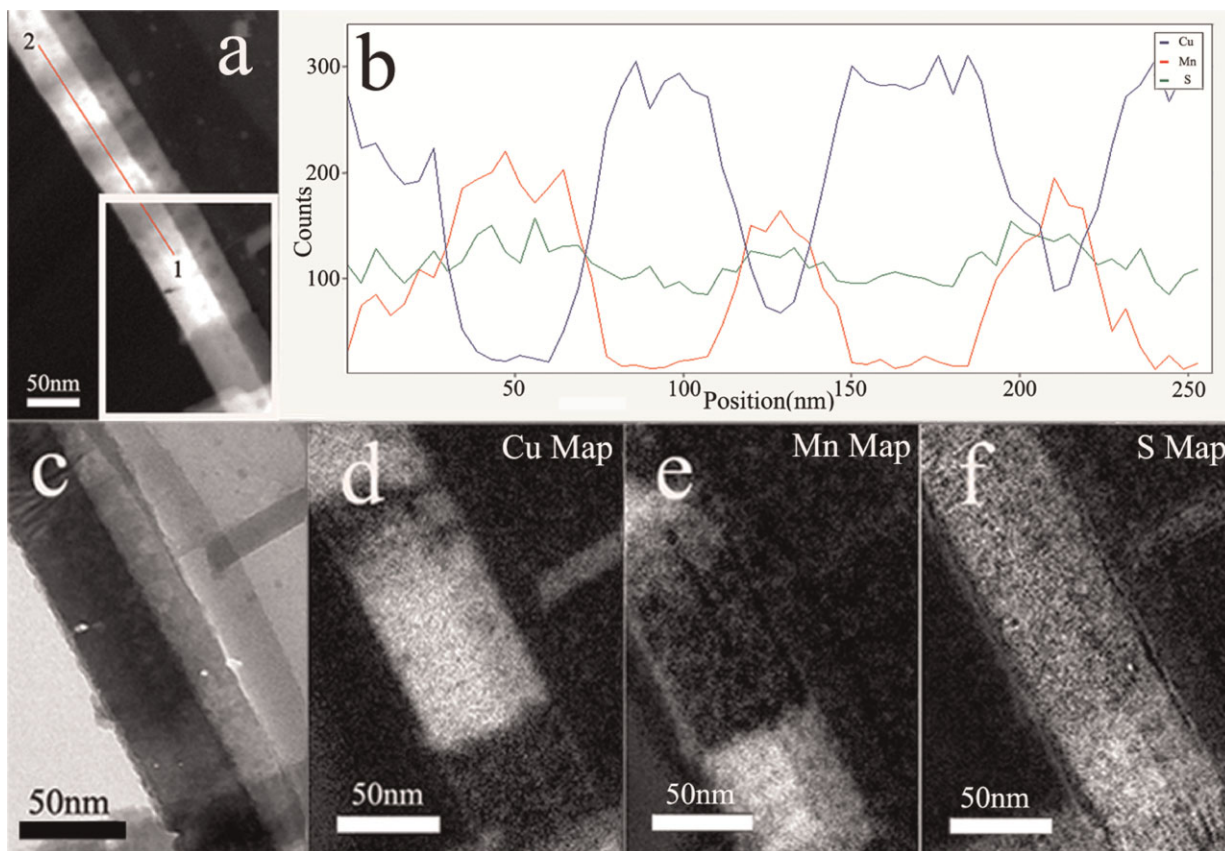
Figure 4 (online color at: www.pss-a.com) (a) HAADF image of a section in MnS/Cu$_2$S heterostructure; (b) plots showing EDS line-scanned composition fluctuation along the red line in (a); (c) EFTEM image of the region marked with the white box in (a); (d–f) element mapping images showing the spatial distribution of Cu, Mn, and S, respectively, along the wire.
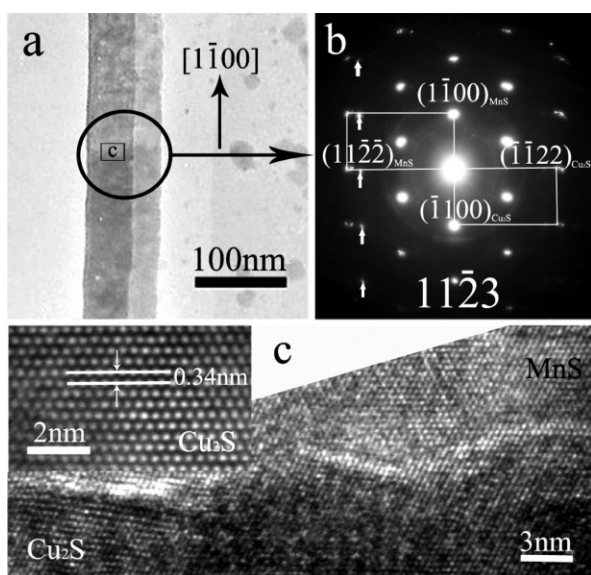
Figure 5 (a) TEM image of a section of MnS/Cu$_2$S heterostructure; (b) SAED pattern taken from the region marked with the black circle in (a); (c) HRTEM image of the area marked with the symbol c in (a), the inset is the enlarged HRTEM image of local Cu$_2$S segment.

arrowheads in Fig. 5b are proposed to result from the weak $[11\text{–}22]_{Cu2S}$ pattern.

The interface between Cu$_2$S and MnS is meandering, as shown in Fig. 5c. The boundary between two sulfides is actually not sharp on the atomic scale, rather the boundary is a zone about tens nanometers in width. The measured interplanar spacing from the HRTEM image (shown in the inset of Fig. 5c), ∼0.34 nm, corresponds to the (1–100) lattice plane of hexagonal Cu$_2$S. In two cases of cation-exchange reaction, the final structures of Cu$_2$S nanowires and MnS/Cu$_2$S heterostructures are both single crystalline but some defects may exist in these structures. Further investigations are in progress to analyze the defects especially on the atomic scale.

4 Discussion In the first-step hydrothermal synthesis, thiourea was used as the sulfur source. Since the release of S^{2-} from thiourea in alkaline aqueous media can be controlled by adjusting the pH value of reaction system, the pH value was controlled at 10 by adding the quantitative ethylenediamine. Mn(CH$_3$COO)$_2$ can be dissolved in alkaline aqueous solution, releasing Mn^{2+}. Once the ionic product of Mn^{2+} and S^{2-} exceeds the solubility product of

Phys. Status Solidi A **208**, No. 1 (2011)

127

MnS, MnS can be precipitated. Thus, the formation of MnS in this hydrothermal process could be expressed as the following:

$$SC(NH_2)_2 + Mn(CH_3COO)_2 \xrightarrow{pH=10, H_2O} MnS. \quad (1)$$
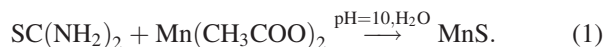
The cation-exchange reactions were performed while immersing γ-MnS nanowires and metal copper in the NaCl aqueous solution under ambient conditions. Under an excess of copper source, the general reaction pathway for the formation of Cu^+ ions in the NaCl aqueous solution can be written as follows:

$$Cu(excess) \xleftrightarrow{Cl^-} Cu^{2+} + 2e^-, \quad (2)$$

$$Cu^{2+} + 2Cl^- + e^- \longleftrightarrow 2CuCl_2^-. \quad (3)$$
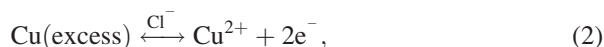
Equations (2) and (3) mean that Cu dissolves as Cu^+ ions in aqueous solution containing Cl^- ions, which is a well-known process reported previously [20]. It is worth noting that the lattice constant of hexagonal Cu_2S is quite close to that of γ-MnS. This excellent topographic superimposition between the S^{2-} anion lattices of Cu_2S and γ-MnS might be responsible for the in and out exchange of Cu^+ and Mn^{2+} cations through the layers of S^{2-} anions without substantial rearrangement of S^{2-} lattices, demonstrating that the following reaction seems to be responsible for the synthesis of Cu_2S nanowires and MnS/Cu_2S heterostructures:

$$MnS + 2Cu^+ \rightarrow Cu_2S + Mn^{2+}. \quad (4)$$

The cation-exchange reaction is considered to be a spontaneous ordering method, where a pattern of nanostructures can emerge naturally due to intrinsic interactions on the nanoscale [21]. In the present study, the factors such as the small size of γ-MnS nanowires, the high mobility of Cu^+, and Mn^{2+} in the crystalline lattices and the solution as the thermodynamic driving forces [3, 5, 7] initiate the nucleation of Cu_2S on γ-MnS nanowire surfaces. The strain fields created by minimizing lattice mismatch [10] between the deposited Cu_2S segments and MnS substrates subsequently yield the ordered Cu_2S nanowires and axial MnS/Cu_2S heterostructures following epitaxial growth. In Fig. 6, the structures of S^{2-} sublattices in wurtzite MnS and hexagonal Cu_2S are presented to show the topotaxial relationship between the reactant and product phases. Anion sublattices show simple epitaxial relationships, where the transformation between different structures can be accomplished by movement of ions mostly in the planes perpendicular to the growth direction (long axis) of γ-MnS nanowire.

The bonding is strongly covalent within the (0001) lattice layer (Fig. 6b) but has a weak van der Waals nature between the {0001} lattice layers for the wurtzite structure (Fig. 6a). Because of the vastly different bonding along the growth direction of these nanowires, one would expect substantially different behaviors, as observed in the case of
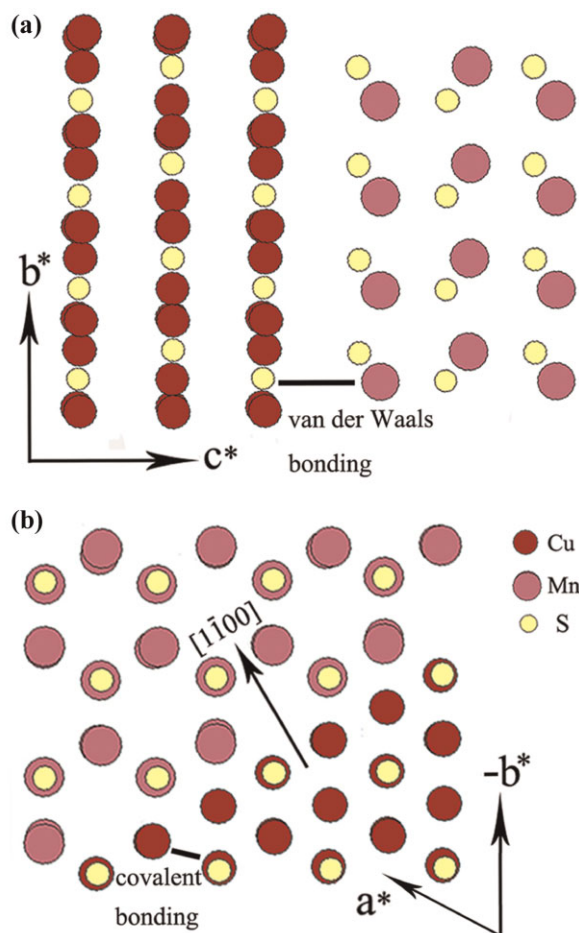
Figure 6 (online color at: www.pss-a.com) Atom configurations of hexagonal Cu_2S and wurtzite MnS, projected from (a) the *a*-axis and (b) the *c*-axis of both phases. Some atoms are at different levels.

anisotropy of chemical transformation from In_2Se_3 to $CuInSe_2$ nanowires through solid-state reaction [22].

The geometry and dimension of the 1D nanostructures were unchanged after the exchange process. The relative rigidity of the anion sublattice enables the partial transformation of nanowire to create a heterostructure where the two compounds share the common anions. In the [0001] γ-MnS nanowires, where the (0001) layer structure is perpendicular to the nanowire long axis, the planar energy with covalent bonding is confined only to the nanowire's cross-section. Cu^+ exchange of Mn^{2+} along [0001] direction just needs to break van der Waals bonding between different loosely held {0001} layers, and there are many free surfaces to serve as ready diffusion sites. It is possible that the entire cation exchange may be accomplished by a small coordinated shear of the layers in the [0001] γ-MnS structure, which are quickly stabilized by diffusion of copper. For the [1–100] γ-MnS nanowires, where the layer structure is parallel to the nanowire long axis, the cation exchange can probably be accomplished by breaking the primary covalent bonding and propagation of a dislocation down the nanowire, a process that would be much slower and need more energy. So, the

diffusion of cation-exchange reaction along the [0001] direction has a higher reaction activity than along the [1–100] direction. The formation of Cu$_2$S nanowires and MnS/Cu$_2$S heterostructures by the axial diffusion suggests that Cu$^+$ has a higher diffusion rate in [0001] γ-MnS nanowires than in [1–100] γ-MnS nanowires.

The mechanism of this selective cation-exchange reaction is attributed to different selective epitaxial diffusion rates along the axial direction in nanowires with different growth directions. It appears plausible that the transformation via selective cation-exchange reaction can also be applied to other nanomaterials.

5 Conclusions We have studied the composition transformation via cation-exchange reaction upon sulfide compounds. By applying cation exchange into γ-MnS nanowires, we found the selectivity of cation-exchange reaction was a function of growth direction of nanowires. In the case of [0001] γ-MnS nanowires, complete conversion into Cu$_2$S nanowires was observed after Cu$^+$ exchange reaction. In contrast, axial MnS/Cu$_2$S heterostructures derived from [1–100] γ-MnS nanowires via epitaxial growth and the orientation relationships of MnS and Cu$_2$S can be identified as $(1–100)_{Cu2S}//(1–100)_{MnS}$ and $[11–23]_{Cu2S}//[11–23]_{MnS}$. The selective exchange of Cu$^+$ in [0001] and [1–100] γ-MnS nanowires is proposed to attribute to different cation-exchange rates along the different growth directions of nanowires. This approach is expected to be applied for preparing various nanojunctions with the desired compositions by the selection of a primary nanostructure configuration.

References

[1] N. Wang, Y. Cai, and R. Q. Zhang, Mater. Sci. Eng. R **60**, 1 (2008).

[2] A. J. Mieszawska, R. Jalilian, G. U. Sumanasekera, and F. P. Zamborini, Small **3**, 722 (2007).

[3] D. H. Son, S. M. Hughes, Y. Yin, and A. P. Alivisatos, Science **306**, 1009 (2004).

[4] Y. Yin, C. Erdonmez, S. Aloni, and A. P. Alivisatos, J. Am. Chem. Soc. **128**, 12671 (2006).

[5] M. V. Kovalenko, D. V. Talapin, M. A. Loi, F. Cordella, G. Hesser, M. I. Bodnarchuk, and W. Heiss, Angew. Chem. Int. Ed. **47**, 3029 (2008).

[6] T. Danieli, N. Gaponik, A. Eychmüller, and D. Mandler, J. Phys. Chem. C **112**, 8881 (2008).

[7] C. Dong and F. C. J. M. van Veggel, ACS Nano **3**, 123 (2009).

[8] P. Hu, D. Jia, Y. Cao, Y. Huang, L. Liu, and J. Luo, Nanoscale Res. Lett. **4**, 437 (2009).

[9] U. Jeong, Y. Xia, and Y. Yin, Chem. Phys. Lett. **416**, 246 (2005).

[10] R. D. Robinson, B. Sadtler, D. O. Demchenko, C. K. Erdonmez, L. Wang, and A. P. Alivisatos, Science **317**, 355 (2007).

[11] K. Lambert, B. De Geyter, I. Moreels, and Z. Hens, Chem. Mater. **21**, 778 (2009).

[12] P. H. C. Camargo, Y. H. Lee, U. Jeong, Z. Zou, and Y. Xia, Langmuir **23**, 2985 (2007).

[13] B. Sadtler, D. O. Demchenko, H. Zheng, S. M. Hughes, M. G. Merkle, U. Dahmen, L. Wang, and A. P. Alivisatos, J. Am. Chem. Soc. **131**, 5285 (2009).

[14] S. E. Wark, C. Hsia, and D. H. Son, J. Am. Chem. Soc. **130**, 9550 (2008).

[15] N. Wang, K. K. Fung, S. Wang, and S. Yang, J. Cryst. Growth **233**, 226 (2001).

[16] Q. Han, J. Zhu, W. Zhu, X. Yang, L. Lu, and X. Wang, Mater. Lett. **63**, 2358 (2009).

[17] Z. L. Wang, Mater. Sci. Eng. R **64**, 33 (2009).

[18] M. E. Anderson, M. R. Buck, I. T. Sines, K. D. Oyler, and R. E. Schaak, J. Am. Chem. Soc. **130**, 14042 (2008).

[19] J. M. Luther, H. Zheng, B. Sadtler, and A. P. Alivisatos, J. Am. Chem. Soc. **131**, 16851 (2009).

[20] T. Ujiro, R. W. Staehle, and W. H. Smyrl, Corros. Sci. **43**, 2185 (2001).

[21] D. O. Demchenko, R. D. Robinson, B. Sadtler, C. K. Erdonmez, A. P. Alivisatos, and L. Wang, ACS Nano **2**, 627 (2008).

[22] D. T. Schoen, H. Peng, and Y. Cui, J. Am. Chem. Soc. **131**, 7973 (2009).